Research Article Vol. 30, No. 25 / 5 Dec 2022 / Optics Express 44896
Optics EXPRESS

Constant hue loci in different color spaces for stimuli in Rec. 2020 color gamut and HDR conditions

HONGBING WANG,[1] MINCHEN WEI,[1,2,*] AND XINCHAO QU[3]

[1]Color, Imaging, and Illumination Laboratory, The Hong Kong Polytechnic University, Kowloon, Hong Kong
[2]Color, Imaging, and Metaverse Research Center, The Hong Kong Polytechnic University, Kowloon, Hong Kong
[3]Dajiang Innovations Technology Co., Ltd., Nanshan, Shenzhen, China
[*]minchen.wei@polyu.edu.hk

Abstract: Hue is an important attribute for characterizing a color stimulus, which is also an output in various color spaces. The investigations on the hue linearity and constant hue loci for different color spaces were generally conducted using conventional CRT displays or surface color samples, in which the color stimuli were within small color gamuts and viewed under standard dynamic range conditions. With the development of imaging technologies, the hue linearity and constant hue loci need to be investigated for wide color gamuts and high dynamic range conditions, which is critically important for image processing (e.g., gamut mapping and tone mapping). In this study, we carefully carried out a hue matching experiment using high-power LED devices. The color stimuli almost reached Rec. 2020 color gamut with the luminance above the diffuse white luminance (i.e., a high dynamic range condition). The results suggested that the hue linearity of IC_TC_P color space was the best among the nine color spaces. Twenty-one constant hue loci were derived for each of these nine color spaces, which can be used for hue correction when performing image processing and to further revise the color spaces.

1. Introduction

Hue is one of the most fundamental dimensions for characterizing the color appearance of a color stimulus. In both the Munsell system and the Natural Color System (NCS), hue is adopted as a dimension to characterize the color appearance of surface colors [1]. For a lot of applications related to color reproduction and processing (e.g., gamut mapping and tone mapping), preserving the hue of a stimulus is always considered the top priority. Thus, hue is commonly defined as one of the three dimensions in most three-dimensional cylindrical color spaces or can be derived directly from Cartesian color spaces.

There are a wide range of color spaces that have been developed and used across various applications, with all the spaces having a lightness axis and a chrominance plane. CIELAB [2] is the most widely used color space, which was mainly developed for conventional applications related to color measurements and specifications. The weaknesses of the CIELAB motivated the development of various better uniform color spaces (e.g., CAM02-UCS [3]). The IPT color space [4] was developed for image-related applications. In order to characterize high dynamic range (HDR) conditions, hdr-CIELAB and hdr-IPT [1] were developed in the 2010s, with IC_TC_P [5] and $J_za_zb_z$ [6] developed recently for also considering wide color gamut (WCG) stimuli. On the other hand, color spaces have also been developed for video-related applications, such as YC_bC_r [7].

A good color space is expected to have good hue linearity, with all the constant hue loci be straight lines converging to the origin of the chrominance planes [1]. This allows to maintain the hue appearance when adjusting the colors along the radial directions or in the same vertical plane

#475433 https://doi.org/10.1364/OE.475433
Journal © 2022 Received 14 Sep 2022; revised 8 Nov 2022; accepted 11 Nov 2022; published 23 Nov 2022

Optics EXPRESS

in the color spaces. Therefore, investigating the hue linearity of color spaces and constant hue loci is of great interest to both the scientific community and the relevant industries, with the hue matching (HM) and the unique hue estimation (UHE) being the two most common methods used in psychophysical experiments.

The HM-based method generally refers to letting observers adjust the color appearance of test stimuli to match the hue appearance of a given reference stimulus, so that a constant hue locus can be derived based on the chromaticities of the adjusted test stimuli and the reference stimulus. For example, Hung and Berns [8] used a CRT display to carry out an HM experiment to derive 12 constant hue loci, which were used to test the hue linearity of four color spaces (i.e., CIELAB, CIELUV, the Hunt model, and the Nayatani model). Ebner and Fairchild [9] also used a CRT display to produce stimuli and derived 15 constant hue loci, which were used to test the hue linearity of CIELAB and CIECAM97s color spaces. The stimuli used in both studies generally had low and medium chroma levels to cover the sRGB color gamut, and suggested the poor hue linearity in the blue hues. Recently, Zhao and Luo [10] carried out an HM experiment using an LCD display to derive the constant hue loci for six hues, and tested the hue linearity of CIELAB, CAM16-UCS, IPT, and $J_za_zb_z$. The stimuli used in this experiment had higher chroma levels and higher luminance than those used in the previous studies. The experiment setup, however, did not provide a strictly WCG and HDR viewing condition, as the stimuli did not reach to Rec. 2020 color gamut [7] and the luminance were lower than the white point luminance.

The UHE method does not require a reference stimulus and relies on the observer's definition of four unitary hues or unique hues (i.e., red, green, blue, and yellow). For example, Xiao et al. [11] used a CRT display to carry out two UHE experiments, and derived constant hue loci for the four unique hues for testing the hue linearity of CIECAM02. Huang et al. [12] and Shamey et al. [13] used Munsell surface color samples to investigate the unique hues and tested the hue linearity in CIELAB, CAM02-UCS, and CIECAM02. The use of Munsell color samples and 8-bit displays, however, always limited the adjustment or selection resolutions, so that the hue intervals between adjacent stimuli were always large. Recently, Bao et al. [14] used a 16-bit project light to produce stimuli with a small hue angle step of 5° and derived the constant hue loci of the four unique hues, which were tested in CIECAM02 and CIELAB color spaces.

The most serious weakness of these past studies was the color range (i.e., color gamut) of the stimuli and the luminance of the stimuli. With the development of HDR imaging technologies, stimuli in a wide color gamut (e.g., Rec. 2020) and a wide range of luminance beyond the diffuse white are becoming more and more common for image reproduction and processing (e.g., gamut mapping and tone mapping). Therefore, the hue linearity for stimuli in Rec. 2020 color gamut and HDR conditions is critically important to different color spaces, and the constant hue loci are urgently needed for processing images.

In this study, we carefully designed an HM experiment, using high-power spectrally tunable LED devices. The color stimuli all had much higher luminance levels than the diffuse white luminance and reached Rec. 2020 color gamut, which was never investigated in the past. A high-resolution control program was developed for allowing the adjustment of the hue angle in a 0.2° step. The hue linearities of nine color spaces that are widely used in practice, including CIELAB [2], CAM02-UCS [3], IPT [4], hdr-CIELAB [1], hdr-IPT [1], YC_bC_r with a non-constant luminance "YC_bC_r (NCL)" [7], YC_bC_r with a constant luminance "YC_bC_r (CL)" [7], IC_TC_P [5], and $J_za_zb_z$ [6], were investigated, and the constant hue loci were derived in these nine spaces.

2. Method

2.1. Apparatus and experimental setup

A viewing booth, whose interiors were painted with Munsell N7 spectrally neutral paint, was used in this study. The booth had dimensions of 70 cm (width) × 45 cm (height) × 60 cm (depth). Three 5 cm × 5 cm openings, with an edge-to-edge distance of 5 cm, were cut on the back wall,

Optics EXPRESS

which were used to produce three color stimuli. On the back side of the back panel, a diffuse black sheet with a reflectance of around 4% was used to cover the right opening and two diffusers were used to cover the left and center openings. Two high-power spectrally tunable LED projection lights were fixed on two tripods placed behind the viewing booth and to illuminate the two diffusers from the back, so that the left and center stimuli appeared to have a uniform and diffuse distribution when viewed from the front side of the viewing booth. These two LED lights were carefully placed, so that the adjustment of one light only affected the corresponding stimulus. Another high-power spectrally tunable LED device was placed above the viewing booth to provide a uniform illumination as the adapting condition. The three LED devices had three chromatic channels (i.e., red, green, and blue) and one warm white channel. The devices were connected in series and controlled using a desktop through a 16-bit Digital Multiplex (DMX) controller, which allowed the intensity of each channel to be individually adjusted. A Gain-Offset-Gamma model was developed for each device to derive the relationship between the 16-bit input signals and the tristimulus values XYZ using the CIE 1931 2° Color Matching Functions (CMFs).

The front side of the viewing booth was partially open, with the upper part covered, so that the observer would not be able to see the LED device placed above the viewing booth directly. A chin rest was placed just outside of the front side of the viewing booth, and centered on the opening. During the experiment, the observer fixed his or her chin on the rest, so that the three stimuli were viewed at the eye height and each stimulus occupied a field of view (FOV) around 5°. Figure 1 shows the experiment setup.

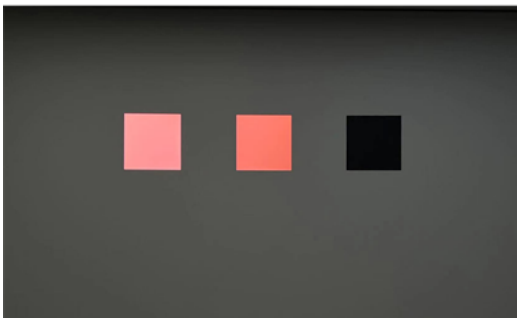

Fig. 1. Photograph of the experiment setup viewed from the observer's eye position during the experiment, with the chin rest removed. The three stimuli from the left to the right are the reference stimulus, the test stimulus, and the black stimulus.

2.2. Adapting condition and stimuli

The device placed above the booth was carefully adjusted to provide an adapting condition with the luminance L_w of 1000 cd/m^2 and the chromaticities of the CIE D65, which was calibrated at the center of the back wall using a PhotoResearch PR-655 spectroradiometer and a Labsphere reflectance standard. The reference and test stimuli were all calibrated to have a luminance of 3400 cd/m^2, so that the viewing condition was an HDR condition.

There were 21 reference stimuli in total, which were designed to have the hue angles uniformly distributed between the three primaries of the LED device in the a^*-b^* plane in the CIELAB color space and to have the highest chroma level, as shown in Fig. 2.

The chroma levels of the test stimuli were selected based on that of the corresponding reference stimulus, so that each reference stimulus had two to four test stimuli at different chroma levels. In total, there were 63 test stimuli. The control program was developed to allow the observer to adjust the hue angle of the test stimulus, with an interval of 0.2°, without changing the chroma and lightness in the CIELAB color space. In order to create an obvious hue difference between

Optics EXPRESS

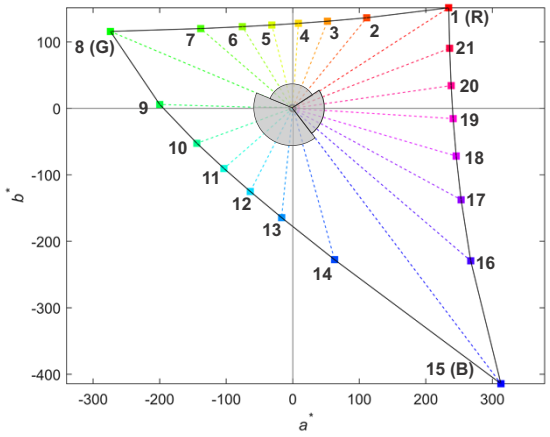

Fig. 2. Chromaticities of the 21 reference stimuli in the a^*-b^* plane of the CIELAB color space, with the color gamut at the luminance of 3400 cd/m^2.

the test and reference stimuli at the beginning, the test stimulus was set to have a hue angle difference of 5° in clockwise in comparison to the reference stimulus. The distribution of the test and reference stimuli in the CIE 1976 $u'v'$ chromaticity diagram, as calibrated and measured using the spectroradiometer, is shown in Fig. 3. It can be seen that the chromaticities of the stimuli were close to the Rec. 2020 color gamut.

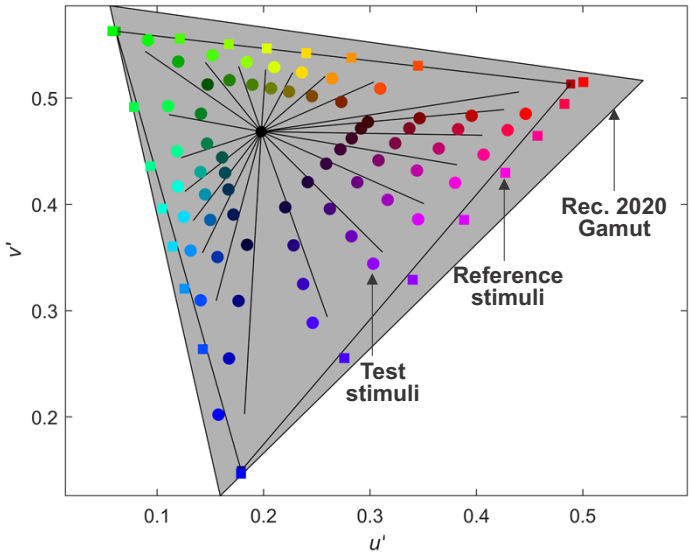

Fig. 3. Chromaticities of the reference and test stimuli, together with the LED device gamut and Rec. 2020 color gamut, in the CIE 1976 $u'v'$ chromaticity diagram. The hue angle of the test stimulus was purposely designed to have a 5° clockwise shift in comparison to the reference stimulus for creating an obvious hue difference. (note: the stimuli were always produced using the warm white channel and two of the three chromatic channels for minimizing the effect of the observer metamerism, so they did not completely cover the color gamut of the LED device.

Optics EXPRESS

It is worthwhile to mention that all the stimuli were produced using the warm white channel and two of the three chromatic channels of the LED devices, so that they had smooth spectral power distributions (SPDs). This was expected to minimize the effect of the observer metamerism [15].

2.3. Observers

Seven observers (four males and three females) between 25 and 34 years of age (mean = 27.71, std. dev. = 2.98) completed the experiment. They all had a normal color vision, as tested using the Ishihara Color Vision Test before the experiment.

2.4. Experimental process

Upon arrival, the observer completed the Ishihara Color Vision Test and a general information survey. The experimenter then escorted the observer to the viewing booth, and explained the concept of hue matching task to him or her. The general illumination in the space was then switched off, and the observer was seated in front of the viewing booth, with his or her chin fixed on the chin-rest.

The observer looked into the viewing booth under the adapting condition for 90 seconds for adaptation. The reference and test stimuli were then presented, and the observer was asked to adjust the color appearance of the test stimulus by rotating a rotary knob clockwise or counterclockwise, until it had the same hue appearance as the reference stimulus. The rotary knob actually changed the hue angle of the test stimulus through the control program. The observer was allowed to take as much time as he or she needed. When he or she was satisfied with the match, the observer pressed a key for confirmation and the control program recorded the signals sent to the LED devices and switched the stimuli to the next pair. The adjustments of four test stimuli, which had the corresponding reference stimuli of 1, 4, 8, and 15 in Fig. 2 and the highest chroma level, were repeated for evaluating the intra-observer variations. Thus, each observer completed the hue matching for 67 pairs of stimuli in a random order.

3. Result and discussion

After the experiment, all the recorded signals were sent to the LED devices to reproduce the adapting condition and the stimuli, with the SPDs of the test stimuli adjusted by each observer measured using the spectroradiometer from the observer's eye position. The measured SPDs were used to derive the various photometric and colorimetric quantities for analyses. In particular, the differences between the measured luminance and target luminance (i.e., 3400 cd/m^2) ranged between -6.77% and -1.06%, with an average of -4.29%, which suggested the control program and LED devices were generally reliable.

3.1. Intra- and inter-observer variations

The intra- and inter-observer variations were characterized using the mean hue angle difference from the mean in the CIELAB color space. In particular, the intra-observer variations were characterized based on the mean differences between the two hue angles and average hue angles adjusted by each observer for the four sets of repeated adjustments, ranging between 0.91° and 1.99°, with a mean of 1.41°. These were significantly smaller than those in the past studies [11,14], suggesting the higher reliability of the adjustments made by the observers.

The inter-observer variations were characterized based on the mean differences between the hue angles of all the 67 adjustments made by each observer and the average hue angles of the 67 adjustments across all the observers (i.e., an average observer), ranging between 4.44° and 9.02°, with a mean of 5.79°. Similarly, the inter-observer variations were also much smaller than those in the past studies [11,14]. In addition, the intra-observer variations were much smaller

Optics EXPRESS

than the inter-observer variations. Figure 4 shows the inter-observer variations, in terms of the hue angle difference, for the 21 reference stimuli. It is clear that the observers had much larger differences in judging the blue hues, which was consistent to various studies investigating the observer metamerism [16], though all the stimuli in this experiment had broadband SPDs.

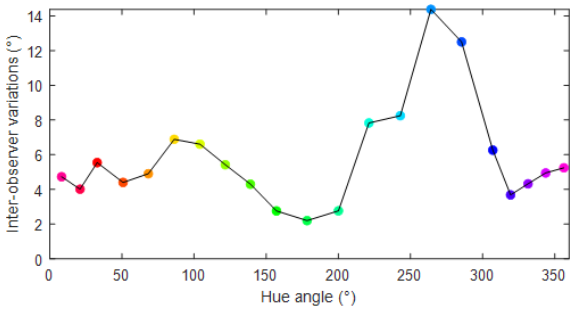

Fig. 4. Relationship between the inter-observer variations, in terms of the hue angle differences, and the hue angles of the 21 reference hues, characterized in the CIELAB color space.

3.2. Hue linearity of different color spaces

The average chromaticities of the test stimuli adjusted by the observers and those of the reference stimuli were calculated in nine different color spaces, which were then used to derive the hue angles for investigating the hue linearity of the nine color spaces.

3.2.1. Hue angle difference and standard deviation of hue angles

The hue angle difference $|\Delta h|$ between each test stimulus and the corresponding reference stimulus was calculated as the most straightforward way to characterize the hue linearity, which was then used to derive the mean hue angle difference $\overline{|\Delta h|}$ for each of the 21 reference stimuli (i.e., hues), as summarized in Fig. 5. On average, CAM02-UCS, IPT, and IC_TC_P were found to have relatively smaller mean of the hue angle differences across the 21 hues, with the values of 3.72, 3.78, and 3.79, while CIELAB and hdr-CIELAB had the worst performance, with the values of 6.37 and 7.19. On the other hand, the blue and red/purple hues generally had the worst hue linearity in most color spaces.

The standard deviation of the hue angles of the stimuli having the same hue appearance is another metric that has been used to characterize the hue linearity. It considers all the test for the same reference stimulus and the reference stimulus itself together and quantifies the variations of the hue angles, as illustrated using Eqs. (1) and (2).

$$SD = \sqrt{\frac{\sum_{i=1}^{N} |h_i - \mu|^2}{N-1}}. \tag{1}$$

$$\mu = \frac{1}{N}\sum_{i=1}^{N} h_i. \tag{2}$$

where N is the number of the test and reference stimuli for each reference stimulus (i.e., hue), h_i is the hue angle of the test or reference stimulus.

Figure 6 shows the standard deviation of the hue angles for each of the 21 reference stimuli (i.e., hues) for the nine color spaces. On average, IC_TC_P and CAM02-UCS had the smallest standard

Optics EXPRESS

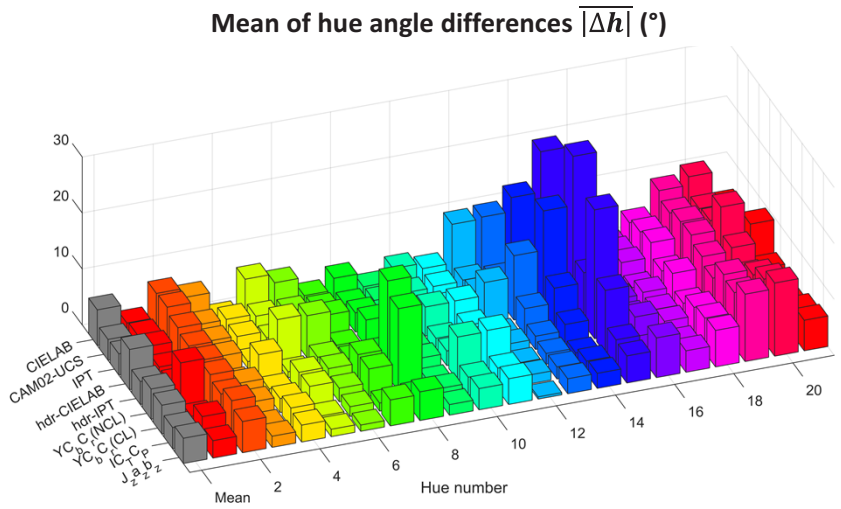

Fig. 5. Summary of the mean of the hue angle differences between the test stimuli and the corresponding reference stimuli for the 21 reference stimuli (i.e., hues) for the nine color spaces.

deviations, with the values of 2.91 and 2.99, while CIELAB and hdr-CIELAB had the largest standard deviations, with the values of 4.60 and 5.00. Similarly, the blue and red/purple hues generally had the largest standard deviations for most color spaces. Such results were consistent to those based on the average hue angle differences presented above.

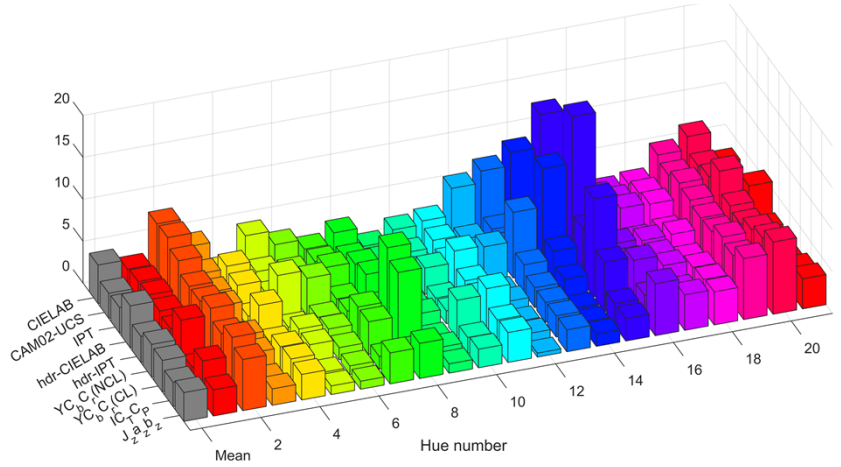

Fig. 6. Summary of the standard deviations of the hue angles of all the test and reference stimuli for each reference stimulus (i.e., hue) for the 21 reference stimuli (i.e., hues) for the nine color spaces.

3.2.2. Root mean square error of hue angle differences

In addition to the above two metrics, the root mean square error (RMSE) of the hue angle differences between each test and its corresponding reference stimulus were calculated for each

Optics EXPRESS

of the 21 reference stimuli (i.e., hues), as illustrated using Eq. (3).

$$RMSE = \sqrt{\frac{\sum_{i=1}^{N} |h_i - h_{ref}|^2}{N}}. \tag{3}$$

where N is the number of the test stimuli for each reference stimulus (i.e., hue), h_{i} is the hue angle of the test stimulus, and h_{ref} is the hue angle of the corresponding reference stimulus.

Figure 7 shows the RMSE value for each of the 21 reference stimuli (i.e., hues) for the nine color spaces. On average, $\mathrm{IC_TC_P}$, CAM02-UCS, and IPT had the best performance, with the values of 4.29, 4.31, and 4.39, while CIELAB and hdr-CIELAB had the worst performance, with the values of 7.10 and 7.93. Similarly, the blue and red/purple hues had relatively large values.

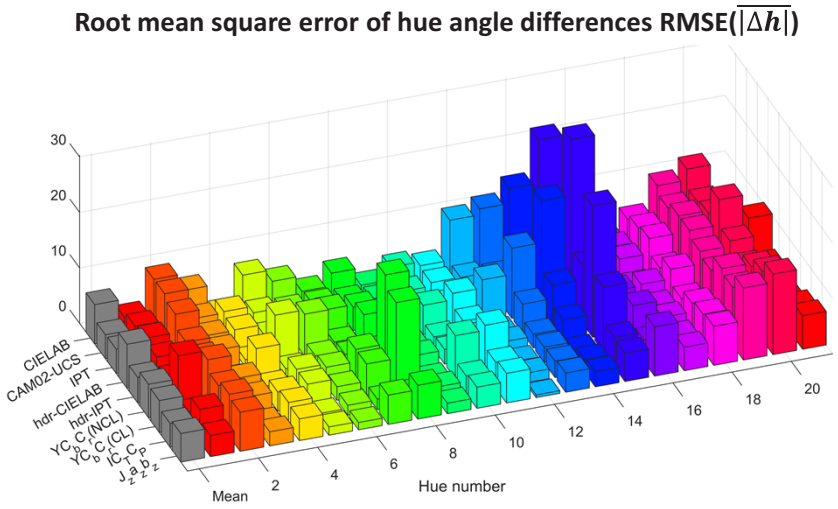

Fig. 7. Summary of the root mean square error of the hue angle differences between the test stimuli and the corresponding reference stimuli for the 21 reference stimuli (i.e., hues) for the nine color spaces.

In general, the above three metrics led to consistent results that $\mathrm{IC_TC_P}$ and hdr-CIELAB had the best and worst performance among the nine color spaces, though both of them were designed for HDR conditions. In contrast, CAM02-UCS and CIELAB had the best and worst performance among those that were not designed for HDR conditions. Furthermore, the bad performance was mainly caused by the blue and red/purple hues.

3.2.3. Perceptual hue differences

Using hue angles to characterize the performance of hue linearity ignores the effect of chroma level, which can be improved using the perceptual hue difference $|\Delta H|$ between the test stimuli and its corresponding reference stimulus, as described using Eq. (4).

$$|\Delta H| = \left| 2\sqrt{C_r C_t} \sin \frac{h_r - h_t}{2} \right|. \tag{4}$$

where C_{r} and C_{t} are the chroma levels of the reference and test stimuli, and h_{r} and h_{t} are the hue angles of the reference and test stimuli. The average perceptual hue differences $\overline{|\Delta H|}$ were then calculated for the 21 reference stimuli (i.e., hues) for the nine color spaces, as shown in Fig. 8

Optics EXPRESS

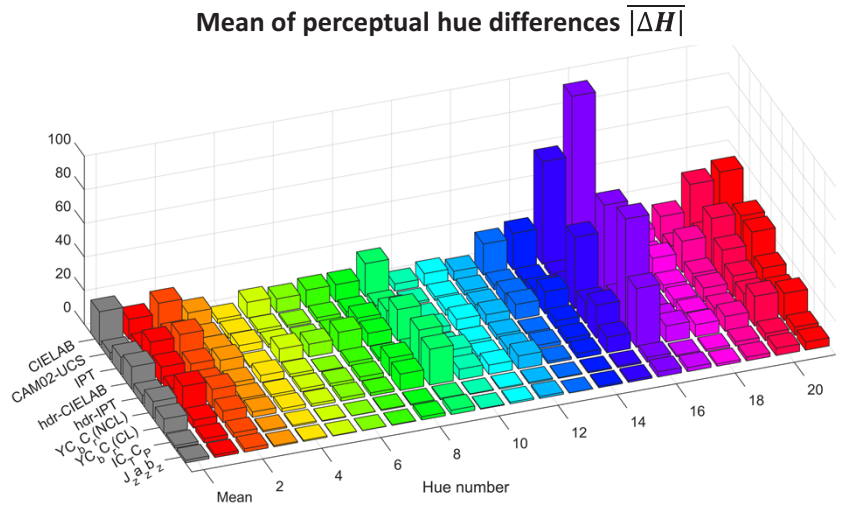

Fig. 8. Summary of the mean of the perceptual hue differences between the test stimuli and the corresponding reference stimuli for the 21 reference stimuli (i.e., hues) for the nine color spaces.

(note: the chroma values in IPT, YC_bC_r (NCL), YC_bC_r (CL), IC_TC_P, and $J_za_zb_z$ were multiplied by 100, allowing the comparisons among the nine color spaces).

It can be observed that IC_TC_P and $J_za_zb_z$ had the best performance, with the values of 1.43 and 1.57, while CIELAB and hdr-CIELAB had the worst performance, which were generally consistent to the results derived from the above three metrics. Also, the bad performance for the blue and red/purple hues were also consistent to those reported above.

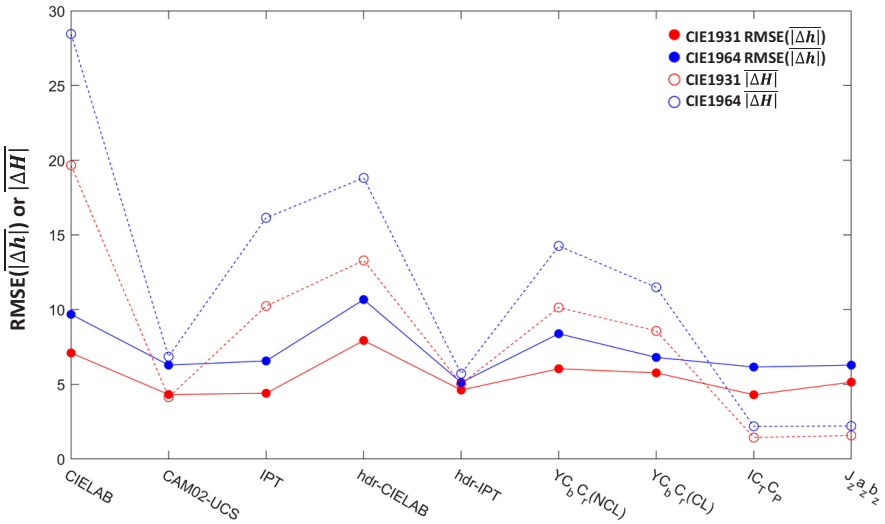

Fig. 9. Comparisons of the mean $RMSE(\overline{|\Delta h|})$ and $\overline{|\Delta H|}$ values derived using the CIE 1931 2° and CIE 1964 10° CMFs for the nine color spaces.

Optics EXPRESS

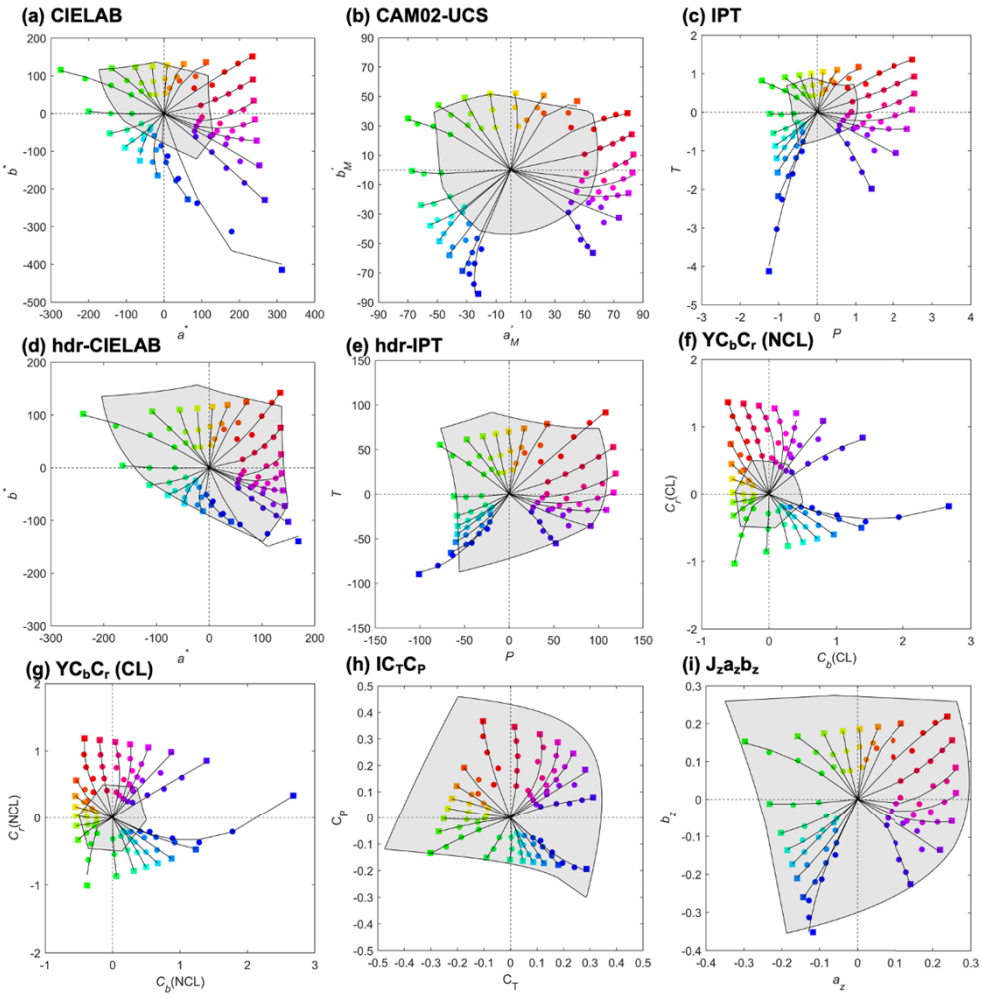

Fig. 10. Average chromaticities of the test stimuli adjusted by the observers and the chromaticities of the reference stimuli in the chrominance plane of nine different color spaces. The curves are the constant hue loci for the 21 hues, which were fitted using a quadratic function based on the chromaticities and the origin. The shaded area is Rec. 2020 color gamut. (a) CIELAB; (b) CAM02-UCS; (c) IPT; (d) hdr-CIELAB; (e) hdr-IPT; (f) YC_bC_r (NCL); (g) YC_bC_r (CL); (h) IC_TC_P; (i) $J_za_zb_z$.

3.3. *Effect of FOV*

All the analyses above, together with the calibrations of the adapting condition, the reference stimuli, and the control program, were designed using the CIE 1931 2° CMFs, which are the most widely used CMFs in image processing and imaging system calibration. The stimuli, however, occupied FOVs of 5° in the experiment, which were not consistent to the CMFs used for calibration and analyses. Therefore, we also used the CIE 1964 10° CMFs to analyze the experiment data, with Fig. 9 showing the comparisons of the $RMSE(\overline{|\Delta h|})$ and $\overline{|\Delta H|}$ values derived using the two CMFs. It can be observed that though the two sets of CMFs caused differences, the overall trends and relationships among the nine color spaces remained the same.

Optics EXPRESS

3.4. Constant hue loci in different color spaces

Based on the average chromaticities of the test stimuli and those of the reference stimuli in the nine color spaces, a quadratic function was used to derive the constant hue loci for the 21 hues in each color space, as shown in Fig. 10. This also clearly shows the hue linearity of the different color spaces for the different hues. The straighter the line is, the better the hue linearity is. It is obvious that IC_TC_P generally had the best performance, but the loci for the blue and purple hues need to be further optimized. In contrast, CIELAB had the worst performance, especially in the blue hues. Such constant hue loci will be extremely useful for making hue corrections when performing tone and gamut mapping on HDR images.

4. Conclusions

A hue matching experiment was carefully designed to investigate the hue linearity for stimuli reaching Rec. 2020 color gamut and viewed under a high dynamic range condition. High-power LED devices were calibrated to produce the D65 adapting condition with a luminance L_w of 1000 cd/m^2 and to produce stimuli at a luminance of 3400 cd/m^2. The observers adjusted the color appearance of a test stimulus to match the hue appearance of a reference stimulus, which was achieved through a customized control program to change the hue angle in a step of 0.2° without changing the lightness and chroma in the CIELAB color space. In particular, the stimuli were produced using a white LED and two chromatic LEDs for minimizing the observer metamerism, resulting in much smaller inter-observer variations. Also, the small hue step resulted in much smaller intra-observer variations, in comparison to past studies.

The test stimuli adjusted by the observers were used to investigate the hue linearity of 21 different hues in nine color spaces that are widely used in practice. IC_TC_P and CIELAB were found to have the best and worst performance respectively, and all the color spaces had relatively worse performance for the blue and red/purple hues. No significant difference was found when the experiment data was analyzed using the CIE 1931 2° or CIE 1964 10° CMFs. Based on the experiment data, 21 constant hue loci were derived for each of the nine color spaces. These can be used for hue corrections when performing image processing (e.g., gamut mapping and tone mapping), and can also be used for further optimizing the color spaces.

Funding. Research Grants Council, University Grants Committee (PolyU 152031/19E).

Disclosures. The authors declare no conflicts of interest.

Data availability. Data underlying the results presented in this paper are not publicly available at this time but may be obtained from the authors upon reasonable request.

References

1. M. D. Fairchild, *Color Appearance Models*, 3rd edition. (John Wiley & Sons, 2013, pp. 450).
2. CIE, "Colorimetry, 4th edition," in *CIE 015*:2018 (CIE, 2018).
3. M. R. Luo, G. Cui, and C. Li, "Uniform color spaces based on CIECAM02 color appearance model," Color Res. Appl. **31**(4), 320–330 (2006).
4. F. Ebner and M. D. Fairchild, "Development and testing of a color space (IPT) with improved hue uniformity," *6th Color and Imaging Conference*, 8–13 (1998).
5. ITU-R Recommendation BT.2100, "Image parameter values for high dynamic range television for use in production and international programme exchange," 2018.
6. M. Safdar, G. Cui, Y. J. Kim, and M. R. Luo, "Perceptually uniform color space for image signals including high dynamic range and wide gamut," Opt. Express **25**(13), 15131–15151 (2017).
7. ITU-R Recommendation BT.2020, "Parameter values for ultra-high definition television systems for production and international programme exchange," 2012.
8. P. C. Hung and R. S. Berns, "Determination of constant hue loci for a CRT gamut and their predictions using color appearance spaces," Color Res. Appl. **20**(5), 285–295 (1995).
9. F. Ebner and M. D. Fairchild, "Finding constant hue surfaces in color space," in *Color Imaging: Device-Independent Color, Color Hardcopy, and Graphic Arts III*, (SPIE, 1998), 107–117.
10. B. Zhao and M. R. Luo, "Hue linearity of color spaces for wide color gamut and high dynamic range media," J. Opt. Soc. Am. **37**(5), 865–875 (2020).

Optics EXPRESS

11. K. Xiao, S. Wuerger, C. Fu, and D. Karatzas, "Unique hue data for colour appearance models. Part I: Loci of unique hues and hue uniformity," Color Res. Appl. **36**(5), 316–323 (2011).
12. H. P. Huang, M. Wei, K. Xiao, and L. C. Ou, "Unique hue judgments using saturated and desaturated Munsell samples under different light sources," Color Res. Appl. **44**(3), 419–425 (2019).
13. R. Shamey, M. Zubair, and H. Cheema, "Unique hue stimulus selection using Munsell color chips under different chroma levels and illumination conditions," J. Opt. Soc. Am. **36**(6), 983–993 (2019).
14. W. Bao, M. Wei, and K. Xiao, "Investigating unique hues at different chroma levels with a smaller hue angle step," J. Opt. Soc. Am. **37**(4), 671–679 (2020).
15. Y. Park and M. J. Murdoch, "Efficiently evaluating the effect of color gamut and spectral bandwidth on observer metamerism in high dynamic range displays," J. Soc. Inf. Disp. **29**(9), 704–722 (2021).
16. J. Wu and M. Wei, "Color mismatch and observer metamerism between conventional liquid crystal displays and organic light emitting diode displays, Part II: adjacent stimuli with a larger field of view," Opt. Express **29**(25), 41731–41744 (2021).